Molecular Therapy
Nucleic Acids
Original Article

Novel Mouse miRNA Chr13_novelMiR7354-5p Improves Bone-Marrow-Derived Mesenchymal Stem Cell Differentiation into Insulin-Producing Cells

Feng Zhao,[1,5] Xiaoyu Liu,[2,5] Zhe Wang,[3] Hongxin Lang,[1] Tao Zhang,[1] Rui Wang,[1] Xuewen Lin,[1] Dan He,[1] Ping Shi,[4] and Xining Pang[1,4]

[1]Department of Stem Cells and Regenerative Medicine, Shenyang Key Laboratory for Stem Cells and Regenerative Medicine, Key Laboratory of Cell Biology, Ministry of Public Health, and Key Laboratory of Medical Cell Biology, Ministry of Education, China Medical University, 77 Puhe Street, Shenbei New District, Shenyang City 110122, Liaoning Province, China; [2]Department of Obstetrics and Gynecology, Center for Assisted Reproduction, Shengjing Hospital of China Medical University, 39 Huaxiang Street, Tiexi District, Shenyang City 110022, Liaoning Province, China; [3]Department of Pathology, Shengjing Hospital of China Medical University, 36 Sanhao Street, Heping District, Shenyang City 110004, Liaoning Province, China; [4]Shenyang Amnion Bioengineering and Technology R&D Center, 155-5 Chuangxin Street, Hunnan District, Shenyang City 110015, Liaoning Province, China

MicroRNAs (miRNAs) that play key roles in the generation of insulin-producing cells from stem cells provide a cell-based approach for insulin replacement therapy. In this study, we used next-generation sequencing to detect the miRNA expression profile of normal mouse pancreatic β cells, non-β cells, bone marrow mesenchymal stem cells (BM-MSCs), and adipose-derived stem cells (ADSCs) and determined relative miRNA expression levels in mouse pancreatic β cells. After the novel mouse miRNA candidates were identified using miRDeep 2.0, we found that Chr13_novelMiR7354-5p, a novel miRNA candidate, significantly promoted the differentiation of BM-MSCs into insulin-producing cells *in vitro*. Furthermore, Chr13_novelMiR7354-5p-transfected BM-MSCs reversed hyperglycemia in streptozotocin (STZ)-treated diabetic mice. In addition, bioinformatics analyses, a luciferase reporter assay, and western blotting demonstrated that Chr13_novelMiR7354-5p targeted Notch1 and Rbpj. Our results provide compelling evidence of the existence of 65 novel mouse miRNA candidates and present a new treatment strategy to generate insulin-producing cells from stem cells.

INTRODUCTION

Type 1 diabetes mellitus (T1D) is a form of diabetes that results from autoimmune-mediated loss of insulin-secreting β cells in the pancreas.[1] Due to its constantly increasing incidence, T1D has become one of the most common chronic diseases of childhood.[2] Replacement of β cells (either through whole pancreas, islet cell transplantation, or insulin-producing cell transplantation) would be the ideal solution to control or reverse diabetes.[3] However, the shortage of donors for pancreas transplantation and the risks associated with organ transplantation are significant obstacles for widespread clinical application.[4,5]

The need for β cell replacement has led to the development of stem cells to generate insulin-producing cells (IPCs) for therapeutic application. Mesenchymal stem cells (MSCs) have the potential to differentiate into a variety of cells in important tissues, including bone, fat, cartilage, myocardium, nerves, and islet cells.[6–10] Because of their immunomodulatory properties and strong capacity for self-renewal and differentiation, MSCs offer an attractive source of stem cells for cell-based therapeutic applications, including for T1D.[11,12] Among all MSC types, bone marrow MSCs (BM-MSCs) are easy to acquire, are associated with no ethical issues, and have unique advantages in autotransplantation.[13,14]

BM-MSCs have great potential to generate IPCs and thus present an attractive source of stem cells for generation of surrogate β cells.[15] Stable expression of key transcription factors, such as Pdx1 and MafA, induces BM-MSCs to differentiate into IPCs.[16,17] Using a three-stage protocol, researchers have successfully generated IPCs from human BM-MSCs in high yields.[18] Generation of IPCs from BM-MSCs could be used as a cell-based approach for insulin replacement therapy.

MicroRNAs (miRNAs) are a large family of highly conserved small non-coding RNAs that play important regulatory roles by regulating a vast number of protein-coding genes.[19] The first discovered islet-specific miRNA was miR-375, which contributes to the development of β cells.[20] Mice lacking miR-375 exhibit more pancreatic α cells and a reduced β cell mass.[21] Recently, many miRNAs have been found to be relevant to pancreatic β cell functions, including

Received 20 April 2019; accepted 2 January 2020;
https://doi.org/10.1016/j.omtn.2020.01.001.

[5]These authors contributed equally to this work.

Correspondence: Xining Pang, PhD, Department of Stem Cells and Regenerative Medicine, Shenyang Key Laboratory for Stem Cells and Regenerative Medicine, Key Laboratory of Cell Biology, Ministry of Public Health, and Key Laboratory of Medical Cell Biology, Ministry of Education, China Medical University, 77 Puhe Street, Shenbei New District, Shenyang City 110122, Liaoning Province, China.
E-mail: pangxining@126.com

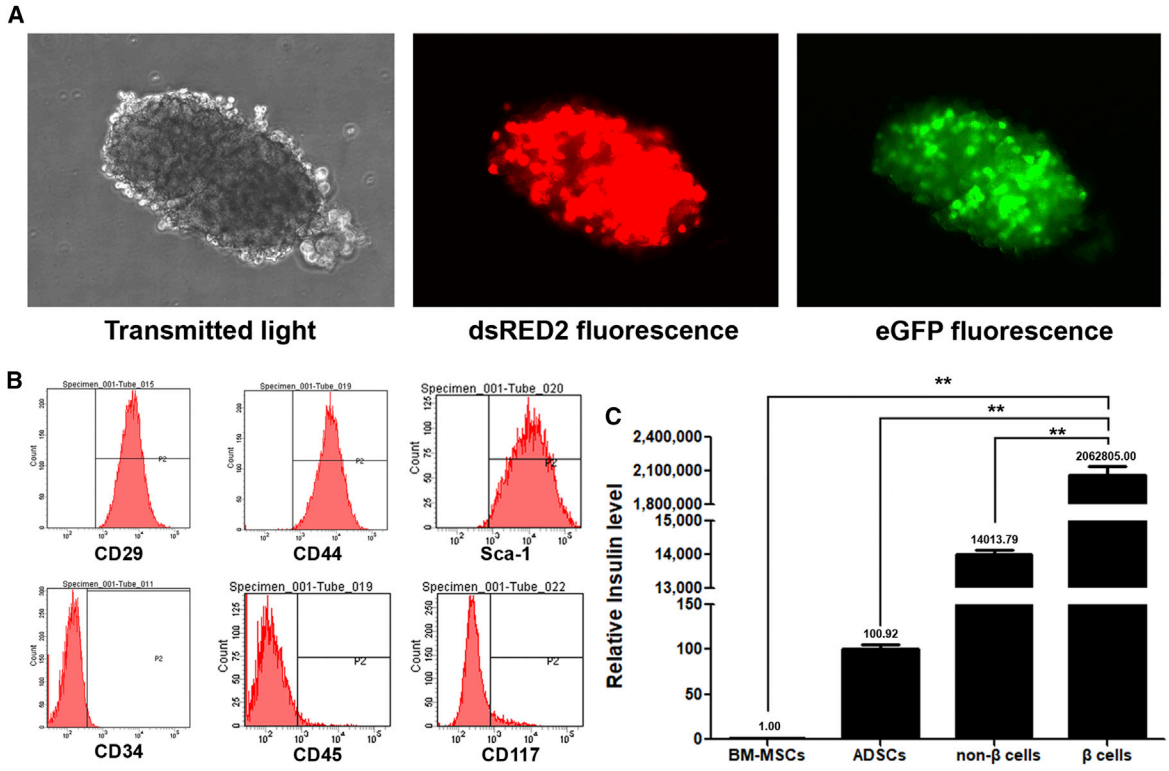

Figure 1. Characterization of Cells *In Vitro*

(A) Pancreatic islets of *Ins*$^{dsRED2+}$/*Ngn3*$^{eGFP+}$ C57BL/6 mice were observed under a fluorescence microscope. Islets were isolated via collagenase digestion and were handpicked under a stereomicroscope. The transmitted light image, Ins-positive cells, and Ngn3-positive cells are shown. (B) Phenotype of ADSCs assessed via flow cytometry analysis. ADSCs were harvested and labeled with antibodies against CD29, CD44, Sca-1, CD34, CD45, and CD117. (C) The Ins2 mRNA levels in BM-MSCs, ADSCs, non-β cells, and β cells were detected via quantitative real-time RT-PCR. The Ins2 level in β cells was significantly higher than levels in the other cells. The results are presented as the means of the values. Bars indicate SD. **$p < 0.01$ for differences between groups.

development, differentiation, survival, insulin production, and insulin secretion.[22] miRNAs, such as miR-34c, miR-375, miR-26a, miR-9, and miR-186, regulate the differentiation of stem cells into IPCs and thus could provide a new treatment strategy for T1D.[23–26]

The MIN6 insulinoma cell line is widely used as a surrogate for mouse pancreatic β cells.[27] In 2013, Baran-Gale et al.[28] performed deep sequencing of miRNAs in MIN6 cells and found that the miRNA expression profile of MIN6 cells is highly correlated with that of primary human β cells. However, the miRNAs expressed in mouse pancreatic β cells under physiologic conditions have not been detected. In this study, we used fluorescence-activated cell sorting to isolate normal pancreatic β cells and pancreatic non-β cells from *Ins*$^{dsRED2+}$/*Ngn3*$^{eGFP+}$ C57BL/6 mice. Using mouse BM-MSCs, adipose-derived stem cells (ADSCs), and non-β cells as the control, we detected the miRNA expression profile of mouse β cells through next-generation sequencing (NGS) and calculated the relative expression levels of miRNAs in mouse β cells. Furthermore, we identified dozens of novel miRNA candidates using miRDeep 2.0[29] and found that Chr13_novelMiR7354-5p (13_7354-5p), a novel miRNA candidate, significantly promotes reprogramming of BM-MSCs into IPCs by targeting Notch1 and Rbpj.

RESULTS

Identification of Cells

After being isolated, pancreatic islets of *Ins*$^{dsRED2+}$/*Ngn3*$^{eGFP+}$ C57BL/6 mice were observed under a fluorescence microscope (Figure 1A). BM-MSCs were characterized as previously described.[17] ADSCs were characterized via flow cytometry analysis, which revealed that the cells expressed Sca-1, CD44, and CD29 and did not express the hematopoietic markers CD117, CD34, and CD45 (Figure 1B). β Cells and non-β cells were separated via fluorescence-activated cell sorting. The Ins2 mRNA levels in BM-MSCs, ADSCs, non-β cells, and β cells were detected using quantitative real-time RT-PCR (Figure 1C). The expression of insulin in β cells was significantly higher than the expression levels in other cells.

Construction of cDNA Libraries and NGS

To investigate differences in miRNA expression between BM-MSCs, ADSCs, non-β cells, and β cells, we prepared cDNA libraries from small RNA extracted from each cell sample and examined the

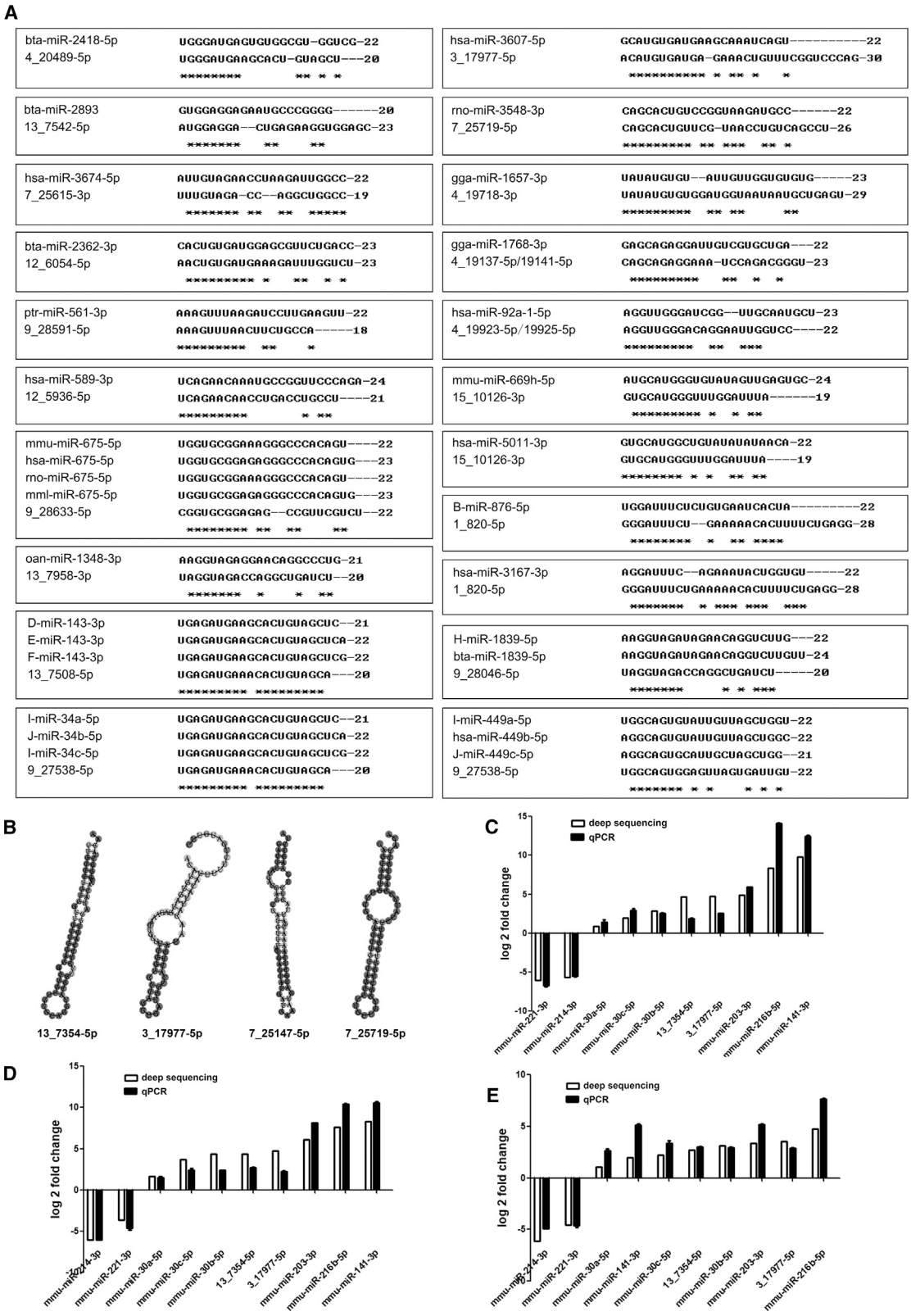

(legend on next page)

miRNA expression levels using NGS with Solexa technology. Among the 20,000,107 total raw reads that were detected in the four samples, 14,881,708 (74.41%) were high-quality reads (18–30 nt). The number of sequence reads that corresponded to known miRNAs was 11,685,228 (78.52% of the high-quality reads), determined by perfect sequence matching to known precursor miRNAs (pre-miRNAs; miRBase release 21) (Table S1). After removal of the matched known miRNAs and other non-coding RNAs, 1,279,193 genome-aligned reads remained for further analyses.

Identification of Novel miRNA Candidates

To uncover potentially novel miRNAs, the reads were analyzed using miRDeep 2.0 software.[29] The results revealed the existence of 267 novel miRNA candidates (Table S2). Among the potential novel miRNA candidates, 65 were detected by at least 10 counts, indicating that they have a high probability of being novel mouse miRNAs (Table S3). Some of the novel miRNA candidates shared seed sequences with known miRNAs in mice and other species (Table S2). 12 candidates (13_7508-5p, 18_13304-3p, 13_7354-5p, 2_14978-5p, 9_28633-5p, 1_820-5p, 9_27538-5p, 6_22759-3p, 6_23472-3p, 9_28046-5p, 13_7958-3p, and 15_10126-3p) shared seed sequences with known mouse miRNAs (mmu-miR-143, mmu-miR-466, mmu-miR-874, mmu-miR-143, mmu-miR-675-5p, mmu-miR-876-5p, mmu-miR-34, mmu-miR-871-3p, mmu-miR-871-3p, mmu-miR-1839-5p, mmu-miR-1839-5p, and mmu-miR-669h-5p), respectively. 6 candidates (15_10126-3p, 9_28633-5p, 1_820-5p, 9_28046-5p, 13_7508-5p, and 9_27538-5p) might be family members of the corresponding known mouse miRNAs because they are conserved miRNAs (Figure 2A). The secondary hairpin structures and minimum free energies of the potential precursors were assessed using RNAfold, and the structures of the selected candidate novel miRNA precursors are shown in Figure 2B.

Differential Expression of miRNAs in β Cells

To validate the expression of miRNAs detected by NGS, we detected the expression of two novel miRNA candidates and eight known miRNAs via qRT-PCR and confirmed the expression (Figures 2C–2E). Correlation analyses showed that the miRNA expression levels detected via NGS had significantly positive correlation with those detected by qRT-PCR (Figure S1). Among all of the known mouse miRNAs and novel miRNA candidates, 61 known miRNAs and 16 novel miRNA candidates were highly expressed in β cells compared with other cells, and 112 known miRNAs and 2 novel miRNA candidates showed low expression levels (Tables S4 and S5).

13_7354-5p Induced BM-MSC Differentiation into IPCs

To further understand the functions of the differentially expressed miRNAs, we predicted target genes of the miRNAs. Four novel miRNA candidates (13_7354-5p, 3_17977-5p, 7_25147-5p, and 7_25719-5p) that were highly expressed in β cells were shown to target genes that inhibit differentiation of MSCs into IPCs. Using Lipofectamine 2000, we transfected BM-MSCs isolated from *Ins*$^{dsRED2+}$/*Ngn3*$^{eGFP+}$ C57BL/6 mice with 13_7354-5p, 3_17977-5p, 7_25147-5p, and 7_25719-5p mimics. The culture medium was exchanged every 72 h. After 8 weeks, the cells were harvested for further experiments. The expression of several genes specific to islet endocrine cells was further detected via qRT-PCR. The mRNA levels of Ins2, Glut2, Ngn3, MafA, NeuroD1, Nkx2.2, and Pdx1 were significantly higher in 13_7354-5p-transfected BM-MSCs than in the negative control (NC) group cells (Figure 3A). As shown in Figure 3B, on day 56 of differentiation, the morphology of the 13_7354-5p-transfected BM-MSCs was islet-like in structure. In addition, the 13_7354-5p-transfected BM-MSCs expressing Ins2 and Ngn3 were observed using fluorescence microscopy. On days 14 and 28 after transfection with 13_7354-5p mimics, the morphology of the 13_7354-5p-transfected BM-MSCs was a β cell-like phenotype, along with less Ins2, which was observed by fluorescence microscopy. However, the formation of cell clusters was not observed (Figure S2).

We further transfected BM-MSCs isolated from wild-type (WT) C57BL/6 mice with 13_7354-5p mimics. The differentiation was performed as described above. Using immunofluorescence staining, we demonstrated that IPCs in the 13_7354-5p group expressed Pdx1, NeuroD1, somatostatin, IAPP, and glucagon on day 56 of differentiation (Figure 4A). In addition, it was detected by western blotting that the endogenous MafA and Nkx2.2 levels showed a clear increment in 13_7354-5p-transfected BM-MSCs on day 56 of differentiation (Figure 4B).

Moreover, ADSCs isolated from *Ins*$^{dsRED2+}$/*Ngn3*$^{eGFP+}$ C57BL/6 mice were transfected with 13_7354-5p mimics. Until day 56 after transfection, the morphology of the 13_7354-5p-transfected ADSCs was not islet-like in structure. Figure S3. In addition, observed by fluorescence microscopy, the 13_7354-5p-transfected ADSCs didn't express Ins2 (Figure S3).

Figure 2. Novel miRNA Candidates

(A) Sequence alignment of novel miRNA candidates with known miRNAs. *, conserved nucleotide; bta, *Bos taurus*; cfa, *Canis familiaris*; eca, *Equus caballus*; gga, *Gallus gallus*; hsa, *Homo sapiens*; mdo, *Monodelphis domestica*; mml, *Macaca mulatta*; mmu, *Mus musculus*; oan, *Ornithorhynchus anatinus*; ptr, *Pan troglodytes*; rno, *Rattus norvegicus*; xtr, Xenopus tropicalis. B, D, E, F, H, I, and J represent the species in which the same miRNAs have the same mature sequence. B represents bta, cfa, eca, hsa, mml, mmu, and rno. D represents cfa, eca, hsa, mml, mmu, and oan. E represents ptr and rno. F represents bta, mdo, and xtr. I represents hsa, mmu, and rno. J represents mmu and rno. H represents cfa, eca, and mmu. (B) Secondary structures of putative precursor hairpins corresponding to four novel miRNA candidates identified in this study. All of these novel miRNAs were expressed at high levels in β cells (see also Table S3). (C) Comparison of qRT-PCR data with NGS data of β cells versus BM-MSCs for 10 miRNAs. The data were transformed into $\log_2$ values of relative expression levels in β cells normalized to U6 snRNA expression levels. (D) Comparison of qRT-PCR data with NGS data of β cells versus ADSCs for 10 miRNAs. The data were transformed into $\log_2$ values of relative expression levels in β cells normalized to U6 snRNA expression levels. (E) Comparison of qRT-PCR data with NGS data of β cells versus non-β cells for 10 miRNAs. The data were transformed into $\log_2$ values of relative expression levels in β cells normalized to U6 snRNA expression levels. The results are presented as the means of the values. Bars indicate SD.

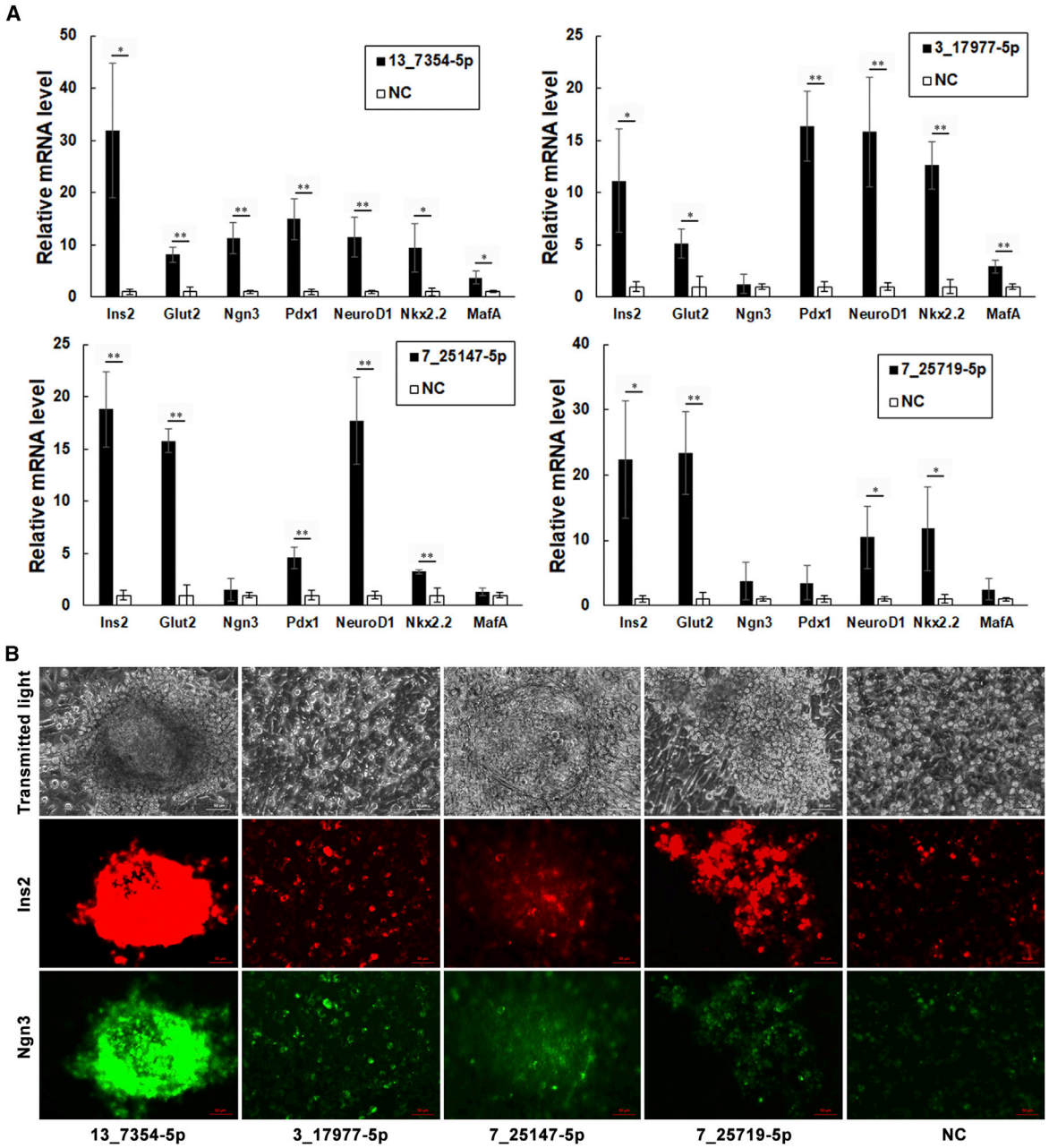

Figure 3. Differentiation of BM-MSCs into IPCs

(A) qRT-PCR was used to detect the mRNA expression levels of Ins2, Glut2, Ngn3, MafA, NeuroD1, Nkx2.2, and Pdx1 from BM-MSCs, which were transfected with 13_7354-5p, 3_17977-5p, 7_25147-5p, and 7_25719-5p mimics and NC. The mRNA levels in cells transfected with NC were defined as 1. The data are presented as the means ± SD of three independent experiments. *$p < 0.05$, **$p < 0.01$ for differences between groups. (B) BM-MSCs isolated from *Ins*$^{dsRED2+}$/*Ngn3*$^{eGFP+}$ C57BL/6 mice were used for differentiation into IPCs. Cells were transfected with 13_7354-5p, 3_17977-5p, 7_25147-5p, and 7_25719-5p mimics and NC. On day 56 of differentiation, cells were observed under a fluorescence microscope. The transmitted light image, Ins-positive cells (red), and Ngn3-positive cells (green) are shown.

Functional Analysis of Differentiated BM-MSCs *In Vitro*

To investigate whether 13_7354-5p improves insulin secretion by IPCs, an ELISA was used to detect insulin and C-peptide secretion from IPCs in response to stimulation with glucose at different concentrations. The results showed that after treatment with 16 and 22 mmol/L glucose, 13_7354-5p-transfected BM-MSCs secreted more insulin and C-peptide than did BM-MSCs in the NC group (Figures 5A and 5B).

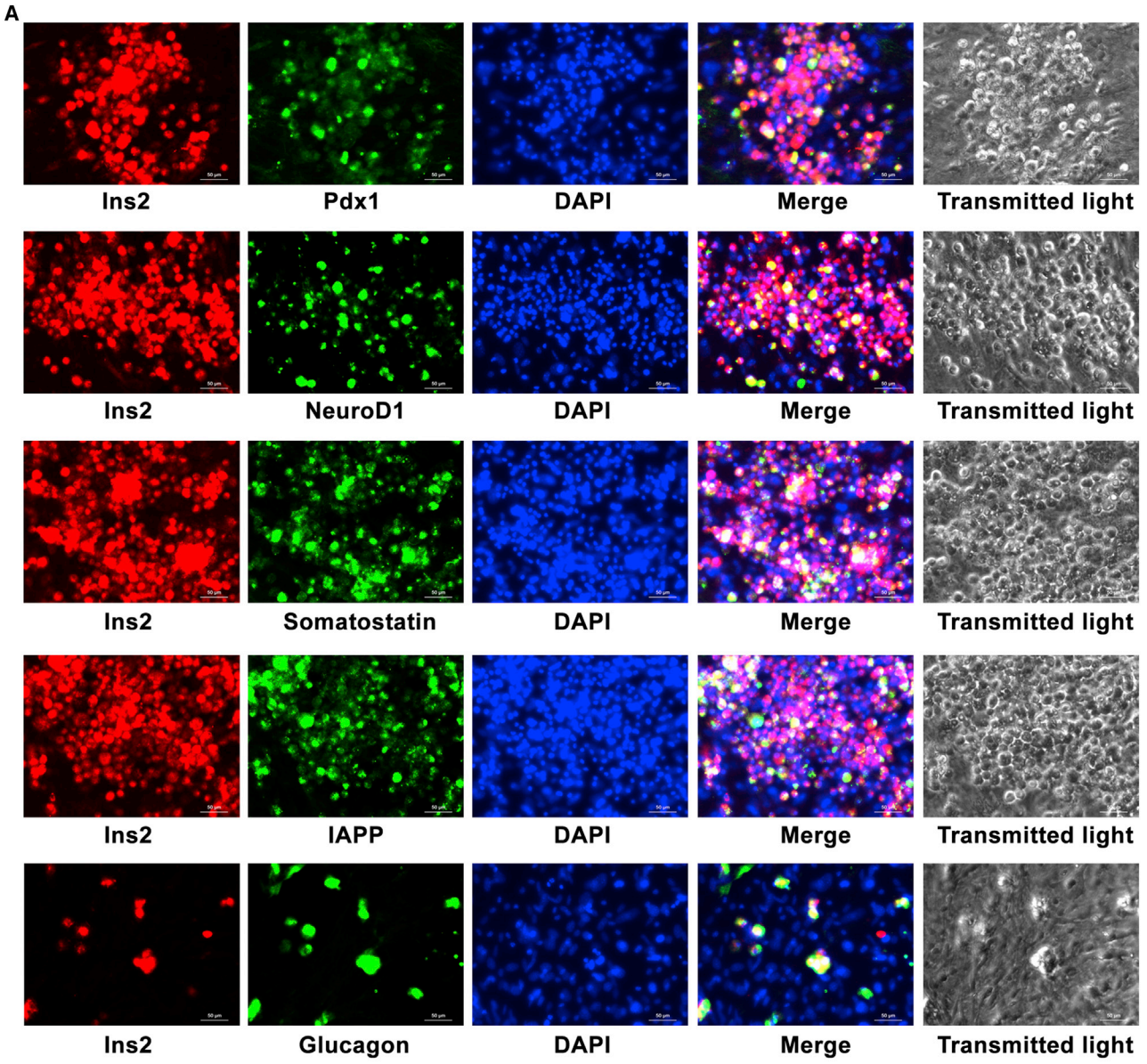

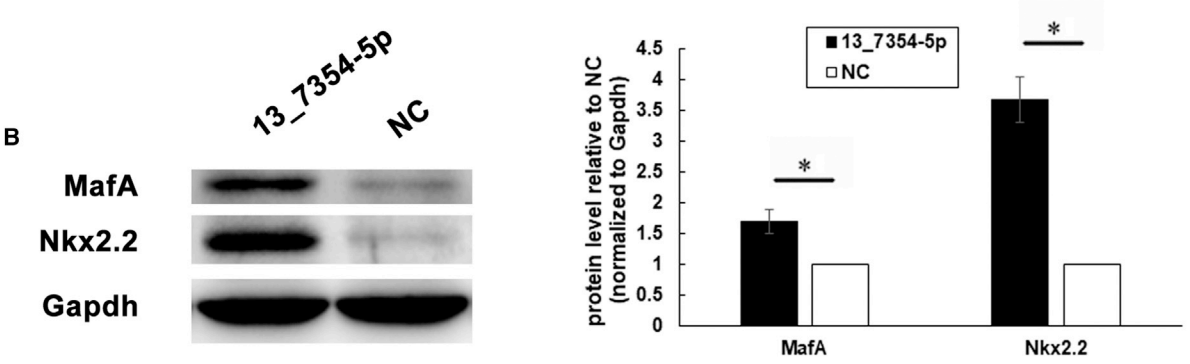

(legend on next page)

After that, we evaluated the insulin and C-peptide secretion under the condition of sequential 2.2 mmol/L glucose, 22 mmol/L glucose, and 30 mmol/L KCl stimulation for 1 h at 37°C. The results showed that after treating with 22 mmol/L glucose and 30 mmol/L KCl, 13_7354-5p-transfected BM-MSCs secreted more insulin and C-peptide than did BM-MSCs of the NC group. In addition, KCl stimulation led to a C-peptide secretion response that was 3-fold greater than glucose stimulation (Figures 5C and 5D).

We further used dithizone (DTZ) staining to evaluate insulin production in IPCs. On day 56 of differentiation, IPCs in the 13_7354-5p group turned red as a result of staining (Figure 5E).

Functional Analysis of Differentiated IPCs *In Vivo*

After transfection with 13_7354-5p mimics or NC, BM-MSCs were transplanted under the left renal capsule of streptozotocin (STZ)-treated diabetic C57BL/6 mice. A clear reduction in blood glucose levels (from greater than 450 mg/dL to approximately 240 mg/dL at 48 days post-transplantation) was found in mice transplanted with 13_7354-5p-transfected BM-MSCs. The blood glucose levels in mice transplanted with NC-transfected BM-MSCs were significantly higher than those in the 13_7354-5p group mice after 24 days post-transplantation. In addition, after removal of the left kidney transplanted with 13_7354-5p-transfected BM-MSCs on day 56, the blood glucose levels rapidly rose to greater than 330 mg/dL, which was significantly higher than the blood glucose levels in mice without removal of the left kidney (Figure 6A). Glucose tolerance tests performed 48 days post-transplantation revealed that differentiated cells were able to respond to the glucose challenge. In mice transplanted with 13_7354-5p-transfected BM-MSCs, the blood glucose levels were significantly lower than those in NC group mice during the course of 2 h after glucose challenge (Figure 6B). These results demonstrate that 13_7354-5p-transfected BM-MSCs reversed hyperglycemia in STZ-treated diabetic mice.

13_7354-5p Targets Notch1 and Rbpj

Using bioinformatics analyses, we found that Notch1 and Rbpj may be potential targets of 13_7354-5p (Figure 7A). To confirm whether these genes are direct targets of 13_7354-5p, we performed a luciferase reporter assay. The results showed that the luciferase activity of pGL3-Notch1-3′ UTR and pGL3-Rbpj-3′ UTR reporters was significantly suppressed in 13_7354-5p-transfected BM-MSCs compared with the activity in NC-transfected BM-MSCs. In contrast, there were no significant differences in the relative luciferase activity of pGL3-Notch1-mutant (MUT) or pGL3-Rbpj-MUT reporters in 13_7354-5p-transfected BM-MSCs compared with the activity in NC-transfected BM-MSCs (Figure 7B).

To further verify these results, we examined the Notch1 and Rbpj protein levels in 13_7354-5p-transfected, NC-transfected, and parental BM-MSCs via western blotting. After normalization to the endogenous reference Gapdh, the endogenous Notch1 and Rbpj levels showed a clear reduction in 13_7354-5p-transfected BM-MSCs (Figure 7C). These results demonstrate that 13_7354-5p may target Notch1 and Rbpj during differentiation of BM-MSCs into IPCs.

DISCUSSION

In pancreatic β cells, many miRNAs, such as miR-7, miR-9, and miR-15, have been shown to be related to insulin synthesis and secretion[22] and found to be differentially expressed in β cells compared with other cells, such as stem cells and pancreatic α cells. However, the miRNAs expressed in mouse pancreatic β cells under physiologic conditions have still not been detected. In this study, we used fluorescence-activated cell sorting to isolate normal pancreatic β cells and pancreatic non-β cells from $Ins^{dsRED2+}/Ngn3^{eGFP+}$ C57BL/6 mice. Furthermore, the miRNA expression profile of mouse β cells was detected via NGS and compared with that of mouse BM-MSCs, ADSCs, and pancreatic non-β cells. Among all of the known mouse miRNAs, 173 known miRNAs were differentially expressed in β cells compared with other cells, including islet-specific miRNA (miR-375).[20] The islet-specific miRNAs miR-7, miR-375, and miR-148a play key roles in pancreatic β cell development and function.[30] Using NGS, we found that mmu-miR-375 and mmu-miR-148a levels in mouse pancreatic β cells were significantly higher than in other cells. In addition, the expression level of mmu-miR-7 in mouse pancreatic β cells and non-β cells was significantly higher than that in MSCs. However, there was no significant difference in mmu-miR-7 expression between β cells and non-β cells. These findings further demonstrate that mmu-miR-375 and mmu-miR-148a are mouse pancreatic β cell-specific miRNAs.

For mammalian miRNA identification, miRDeep 2.0 is commonly used to discover novel miRNAs based on NGS data.[29,31] Using the miRDeep 2.0 program, we identified 65 novel miRNA candidates that have a high probability of being novel mouse miRNAs. Among these miRNAs, 16 novel miRNA candidates were highly expressed in β cells compared with other cells. To uncover miRNAs that promote reprogramming of BM-MSCs into IPCs, we predicted target genes of these miRNAs using bioinformatics analyses and found four novel miRNA candidates (13_7354-5p, 3_17977-5p, 7_25147-5p, and 7_25719-5p) that may target genes that inhibit differentiation of MSCs into IPCs.

To further understand the functions of these miRNAs, we transfected BM-MSCs with 13_7354-5p, 3_17977-5p, 7_25147-5p, and

Figure 4. Differentiation of 13_7354-5p-Transfected BM-MSCs into IPCs

(A) BM-MSCs isolated from WT C57BL/6 mice were transfected with 13_7354-5p. Immunofluorescence analysis was used to detect the expression of Ins2, Pdx1, NeuroD1, IAPP, somatostatin, and glucagon in differentiated 13_7354-5p-transfected BM-MSCs on day 56 of differentiation. DAPI was used for nuclear staining. (B) The protein expression levels of MafA and Nkx2.2 in 13_7354-5p-transfected BM-MSCs relative to NC-transfected BM-MSCs were detected on day 56 of differentiation via western blotting. After normalization to the endogenous reference Gapdh, the endogenous MafA and Nkx2.2 levels showed a clear increment in 13_7354-5p-transfected BM-MSCs. The results are presented as the means of the values. Bars indicate SD. *$p < 0.05$ for differences between groups.

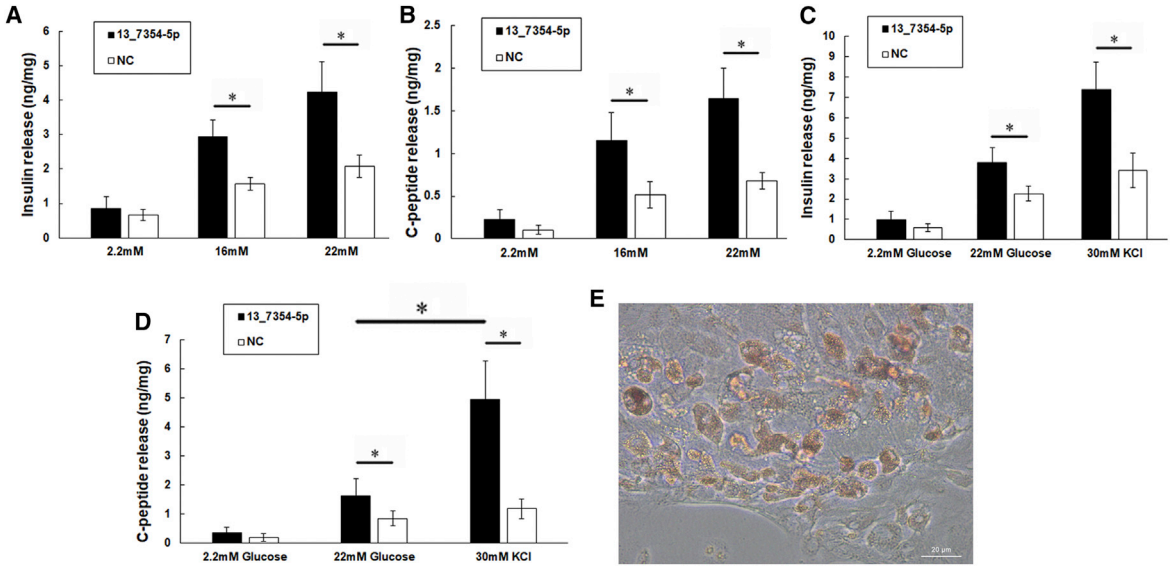

Figure 5. Functional Analysis of Differentiated BM-MSCs *In Vitro*

(A) Insulin levels in response to 2.2, 16, and 22 mmol/L glucose were determined in differentiated 13_7354-5p-transfected BM-MSCs on day 56 via ELISA. BM-MSCs transfected with NC were used as a negative control. (B) C-peptide levels in response to 2.2, 16, and 22 mmol/L glucose were determined in differentiated 13_7354-5p-transfected BM-MSCs on day 56 via ELISA. BM-MSCs transfected with NC were used as a negative control. (C) Insulin secretion of differentiated 13_7354-5p-transfected BM-MSCs on day 56 was detected under the condition of sequential 2.2 mmol/L glucose, 22 mmol/L glucose, and 30 mmol/L KCl stimulation for 1 h at 37°C via ELISA. BM-MSCs transfected with NC were used as a negative control. (D) C-peptide secretion of differentiated 13_7354-5p-transfected BM-MSCs on day 56 was detected under the condition of sequential 2.2 mmol/L glucose, 22 mmol/L glucose, and 30 mmol/L KCl stimulation for 1 h at 37°C via ELISA. BM-MSCs transfected with NC were used as a negative control. (E) Zinc staining in differentiated 13_7354-5p-transfected BM-MSCs on day 56. Cell clusters stained positively for zinc are shown by distinct red staining. The results are presented as the means of the values. Bars indicate SD. *$p < 0.05$ for differences between groups.

7_25719-5p mimics. On day 56 of differentiation, using qRT-PCR, we demonstrated that the mRNA levels of Ngn3, endocrine islet markers (including NeuroD1 and Nkx2.2),[32] and β cell markers (including Ins2, Glut2, MafA, and Pdx1) were significantly higher in 13_7354-5p-transfected BM-MSCs than in NC group cells.[33] In addition, the 13_7354-5p-transfected BM-MSCs could be induced to differentiate into islet-like cells *in vitro* and express Ins2 and Ngn3. As a transcription factor, Ngn3 is critical for endocrine lineage specification and differentiation[34] and is expressed in endocrine progenitor cells. During the pancreas development process, Ngn3 acts as a switch. Researchers have found that Ngn3-positive cells give rise to all islet lineage cells.[35] Overall, these findings demonstrate that 13_7354-5p increases the expression of Ngn3 and promotes the differentiation of BM-MSCs.

Pdx1 and NeuroD1 are key transcription factors in pancreatic cell differentiation.[36] Pdx1 is observed in a single dorsal pancreatic bud around gestational week 4 in humans[37] and is required for early embryonic development of the pancreas and subsequent differentiation of pancreatic lineages.[34] Pdx1 deficiency blocks further pancreatic development and leads to a severe diabetic phenotype in mice.[38] NeuroD1 has also been found to bind to the insulin promoter to induce insulin production[39] and to directly interact with Pdx1 and forms a transcriptional activation complex on the insulin promoter.[34] Using immunofluorescence staining, we demonstrated that IPCs in the 13_7354-5p group expressed Pdx1 and NeuroD1. We think that 13_7354-5p improves insulin expression in IPCs by upregulating the transcription factors Pdx1 and NeuroD1.

We further examined whether 13_7354-5p improves insulin release in response to glucose stimulation. As confirmed by ELISA, insulin secretion by 13_7354-5p group IPCs was significantly higher than that by NC group cells. In addition, we demonstrated that 13_7354-5p-transfected BM-MSCs reversed hyperglycemia in STZ-treated diabetic mice *in vivo*.

During embryonic development, one of the major regulatory networks in control of pancreatic endocrine lineage development is the Notch signaling pathway.[40] The Notch pathway includes a family of conserved transmembrane receptors (Notch 1, 2, 3, and 4) that interact with specific ligands (Delta-like 1, 2, and 3 and Serrate 1 and 2) to regulate cell fate decisions, including proliferation, differentiation, and cell survival.[41,42] Notch signaling acts as an inhibitor of induced β cell differentiation.[36,43,44] It has been found that Notch1 inhibits differentiation of enteroendocrine precursor cells into islet β cells via Rbpj and Hes-1, which leads to downregulation of Ngn3 and NeuroD1.[45] Inhibition of the Notch pathway results in differentiation of insulin-positive progenitors into islets and β cell neogenesis from acinar cells.[36,44] In this study, we demonstrated that Notch1 and Rbpj are direct targets of 13_7354-5p. Moreover, 13_7354-5p

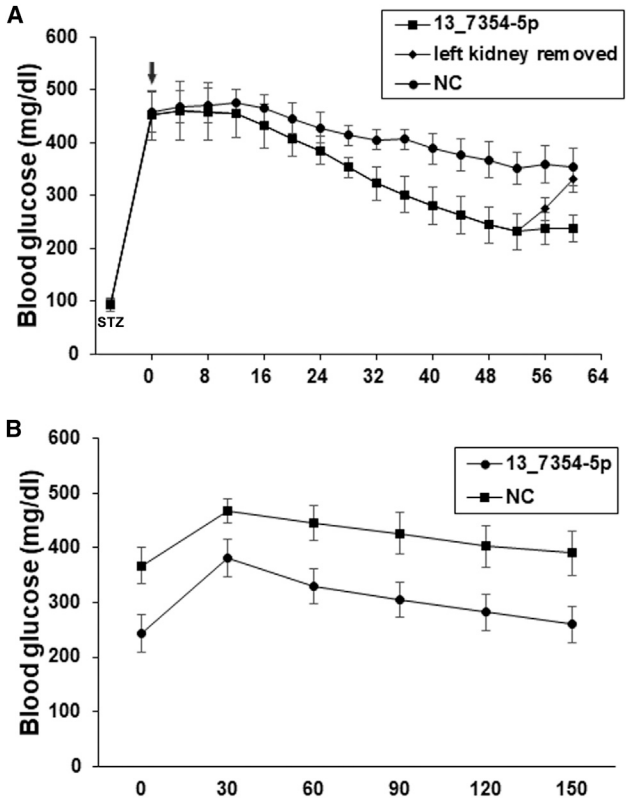

Figure 6. Functional Analysis of Differentiated BM-MSCs *In Vivo*

(A) BM-MSCs transfected with 13_7354-5p mimics or NC were transplanted into STZ-treated diabetic mice whose glucose levels had reached 350 mg/dL. The arrow shows the day of implantation (day 0). Glucose levels were monitored every 4 days. On day 52, the left kidney implanted with differentiated BM-MSCs was removed (n = 3). (B) Glucose tolerance was tested in mice 48 days after transplantation. The blood glucose levels peaked in 0.5 h after taking glucose and returned to normal in 2 h. The results are presented as the means of the values. Bars indicate SD.

promotes the β cell differentiation program through modulation of Notch1 and Rbpj, which in turn inhibits differentiation into β cells via the Notch pathway.

In conclusion, we used NGS to detect miRNA expression in normal pancreatic β cells compared with mouse BM-MSCs, ADSCs, and non-β cells and found that the potentially novel mouse miRNA 13_7354-5p is a mouse pancreatic β cell-specific miRNA. Moreover, 13_7354-5p was found to improve BM-MSC differentiation into IPCs by targeting the Notch1- and Rbpj-induced Notch pathway.

MATERIALS AND METHODS

Experimental Animals

WT C57BL/6 mice (7–10 weeks old) were obtained from Vital River Laboratory Animal Technology (Beijing, China). *Ins*$^{dsRED2+}$/*Ngn3*$^{eGFP+}$ C57BL/6 mice were a kind gift from the Centre for Medical Research, University of Western Australia. All animals were housed in the animal care facilities of China Medical University under specific pathogen-free (SPF) conditions.

Mouse Islet Isolation and Cell Collection

Ins$^{dsRED2+}$/*Ngn3*$^{eGFP+}$ C57BL/6 mice (10–12 weeks old) were used for mouse pancreatic islet isolation. Islets were isolated via collagenase digestion, handpicked under a stereomicroscope, and maintained in 11.1 mmol/L glucose/RPMI 1640 (Thermo Fisher Scientific, Madrid, Spain) supplemented with 10% fetal bovine serum (FBS; HyClone, Logan, UT, USA).[46] Isolated islets were gently dissociated with trypsin (Gibco), resuspended in PBS supplemented with 25 mmol/L HEPES (*N*-2-hydroxyethylpiperazine-*N*′-2-ethanesulfonic acid) and 2.5 mmol/L EDTA, and filtered through a 70-μm cell strainer (Falcon). β Cells (dsRED2^{+}) and non-β cells (dsRED2^{-}) were separated via fluorescence-activated cell sorting (FACS; Astrios Sorter [Beckman Coulter]) based on the fluorescence intensity and wavelength and the size of individual cells.

Cells and Cell Culture

Subcutaneous adipose tissue was obtained from mice (6–8 weeks old) for primary mouse ADSC cultures. The adipose tissue was resected, washed with PBS, and then minced into small pieces. The adipose tissue pieces were digested in DMEM/F-12 medium containing 1 mg/mL collagenase type I (Sigma-Aldrich, St. Louis, MO, USA) for 30 min at 37°C. The cell suspension was filtered through a 70-μm nylon cell strainer, followed by centrifugation in DMEM/F-12 supplemented with 10% FBS. The pellet was resuspended in DMEM/F-12 medium supplemented with 10% FBS, 10 ng/mL murine fibroblast growth factor-basic (M-FGF-b), 100 U/mL penicillin, and 100 μg/mL streptomycin and incubated at 37°C in a humidified incubator with 5% CO_2. When the cells reached 80%–90% confluence, they were passaged for expansion. For the experiments, mouse ADSCs were used at passages 3–6.

To confirm mesenchymal stem cell characteristics, ADSCs at passage 3 were released via trypsinization. After trypsin neutralization with serum-containing medium, the cells were incubated with monoclonal phycoerythrin (PE)-conjugated antibodies against Sca-1, CD29, CD44, and CD73 (BioLegend). Flow cytometry analysis was performed as previously described.[47] Rat immunoglobulin (Ig)G2a or IgG2b conjugated to PE was used as a negative control.

The isolation, culture, and identification of mouse BM-MSCs were performed as previously described.[17]

Construction of cDNA Libraries from Small RNA and NGS

Total RNA from cells was extracted as described previously.[48] For cDNA library construction, total RNA from each sample was sequentially ligated to 3′ and 5′ small RNA adapters. cDNA was synthesized and amplified using Illumina's proprietary RT primers and amplification primers. The amplified samples were purified and size-selected from the PAGE gel. The libraries were quantified with an Agilent 2100 Bioanalyzer. Cluster generation was performed on an Illumina cBot using a TruSeq Rapid SR cluster kit (Illumina). Sequencing

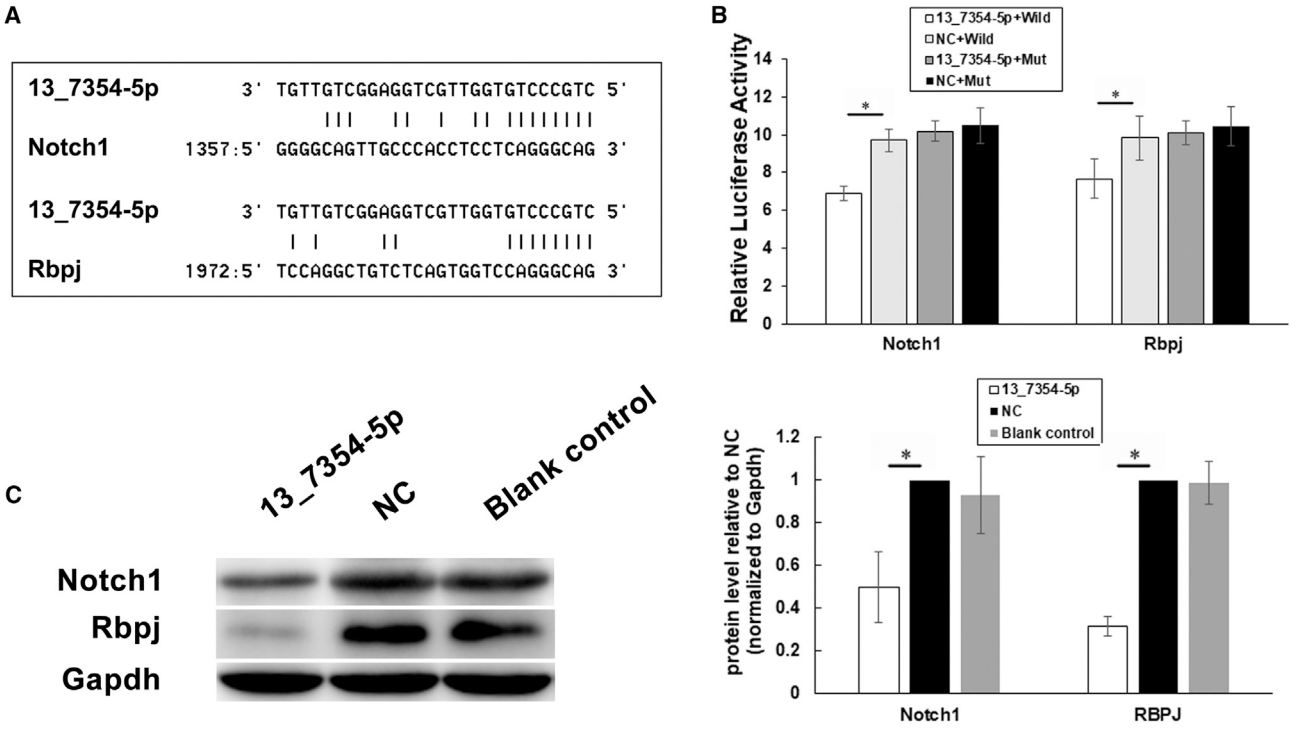

Figure 7. Notch1 and Rbpj Are Directed Targets of 13_7354-5p

(A) Prediction of potential target genes of 13_7354-5p via bioinformatics analyses. The 3′ UTRs of the genes were obtained from both the Ensembl and miRanda databases. (B) Analysis of luciferase activities of Notch1, Rbpj, Notch1-MUT, and Rbpj-MUT with 13_7354-5p mimics or NCs in BM-MSCs. (C) Protein expression analysis of Notch1 and Rbpj in transfected and parental BM-MSCs on day 7 after transfection was detected by western blotting. After normalization to the endogenous reference Gapdh, the endogenous Notch1 and Rbpj levels were clearly reduced in 13_7354-5p-transfected BM-MSCs. The results are presented as the means of the values. Bars indicate SD. *$p < 0.05$ for differences between groups.

was performed on an Illumina HiSeq 2000 system using TruSeq Rapid SBS kits (Illumina). For multiplex sequencing, 36 cycles of a single read were used to sequence the small RNAs. Image analysis and base calling were performed using the Illumina instrument software.

Analysis of Sequence Data

After adaptor sequences and low-quality reads were removed, the high-confidence trimmed reads were aligned to known pre-miRNAs available in miRBase (release 21) to obtain sequences that either matched or did not match known miRNAs.[49] We screened the unmatched reads against Rfam (release 11.0),[50] SILVA 115,[51] and Repbase (version 20.04)[52] to remove contamination from mouse non-coding RNAs, such as small nuclear RNAs (snRNAs), small nucleolar RNAs (snoRNAs), rRNAs, repeat-associated small interfering RNAs (rasiRNAs), and tRNAs. The unmatched reads were then aligned to the mouse GRCm38 genome in Ensembl to filter out the reads in which the linker sequences were either mutated or absent. For mouse miRNA prediction, we used miRDeep 2.0 software to identify novel miRNA candidates and then filter out the sequence reads with a frequency of fewer than 10 counts. The pre-miRNA sequences were mapped to the mouse genome (mouse genome GRCm38/mm10, UCSC Genome Browser) to identify reads with perfect matches. The minimum free energies and the secondary structures of the potential precursors were assessed using the Vienna RNAfold web server (http://rna.tbi.univie.ac.at/). The conservation and potential target genes of miRNAs were predicted as described previously.[48] The Notch signaling pathway was obtained from KEGG (http://www.genome.jp/kegg/). To compare the expression levels of miRNAs between BM-MSCs, ADSCs, non-β cells, and β cells, digital expression profiling based on TPM (transcript reads per million mapped reads) was implemented in the R package edgeR.[53] In this study, we selected differentially expressed miRNAs based on fold change >2 and TPM >10.

Small RNA Preparation and Quantitative Real-Time RT-PCR

Quantitative real-time RT-PCR was used to confirm the expression levels of miRNAs and mRNAs. Total RNA, including small RNA, was extracted using a miRNeasy mini kit (QIAGEN) according to the manufacturer's instructions. The concentration and purity of RNA were assessed via ultraviolet spectrophotometry (ratio of absorbance at 260 and 280 nm [A260/A280] >1.9) using a Thermo Scientific NanoDrop 2000c spectrophotometer. Reverse transcription was performed using a miScript II RT kit (QIAGEN) according to the manufacturer's instructions. Using a miScript SYBR Green PCR kit (QIAGEN), quantitative real-time RT-PCR was performed on an

ABI 7500 real-time PCR system (Applied Biosystems) supplied with analytical software. Known miRNAs were detected using miR-30a-5p, miR-30b-5p, miR-30c-5p, miR-221-3p, miR-214-3p, miR-203-3p, miR-216b-5p, and miR-141-3p miScript primer assays (QIAGEN). U6 and Gapdh RNA levels, endogenous references for miRNAs and mRNAs, respectively, were used for normalization. After the final cycle, a melting curve analysis was conducted within a range of 55°C–95°C. The relative expression miRNA and mRNA levels were calculated as described previously.[48] Primers for RT-PCR are given in Table S6.

Transfection

BM-MSCs were plated 1 day before transfection and transfected with 2′-*O*-methyl oligonucleotides, including 13_7354-5p, 3_17977-5p, 7_25147-5p, and 7_25719-5p mimics and a stable NC (Table S7; GenePharma, China), using Lipofectamine 2000 (Thermo Fisher Scientific) according to the manufacturer's instructions. After 48 h, the cells were harvested for further experiments.

Immunofluorescence Staining

Immunofluorescence staining was performed as previously described.[17] Briefly, at room temperature, cells were fixed with 4% formaldehyde for 30 min and then treated with 0.25% Triton X-100 in PBS for 10 min. After being blocked with 10% normal donkey serum containing 1% BSA in PBS, cells were incubated with primary antibodies against Ins2 (1:200; Cell Signaling Technology), NeuroD1 (1:200; Santa Cruz), or Pdx1 (1:1,000; Abcam) at 4°C overnight. Fluorescence-labeled secondary antibodies were used for detection (Thermo Scientific). Nuclei were stained with DAPI (1 mg/mL; Roche). Images were acquired via fluorescence microscopy.

Measurement of Insulin and C-Peptide Secretion via ELISA

Cells were cultured in serum-free medium containing 0.5% BSA for 12 h. After being washed with PBS, cells were preincubated with Krebs-Ringer bicarbonate (KRB) buffer for 1 h, followed by incubation with KRB buffer containing 2.2, 16, or 22 mmol/L glucose for 1 h at 37°C. For KCl stimulation, the cells were subsequently incubated with 2.2 mmol/L glucose, 22 mmol/L glucose, and 30 mmol/L KCl stimulation for 1 h at 37°C. The supernatant was collected for ELISA (R&D Systems) according to the manufacturer's instructions. Total protein concentration was determined with a BCA protein assay kit.

Dithizone Staining

Staining culture medium containing dithizone (100 μg/mL, Sigma-Aldrich) was used for dithizone staining. Following the addition of dithizone, the dishes were incubated at 37°C for 30 min and then washed three times with PBS. The stained cells were examined microscopically.

Cell Transplantation

All experimental procedures involving animals were in accordance with the *Guide for the Care and Use of Laboratory Animals* and were performed according to the institutional ethical guidelines for animal experiments (as shown in the Supplemental Information). The diabetic mouse model was constructed as previously described.[17] Then, 5×10^6 cells were transplanted under the left renal capsule of diabetic mice. Fasting blood glucose levels were measured every 4 days after transplantation. Glucose tolerance tests were performed as previously described.[17]

Luciferase Reporter Assay

For luciferase reporter experiments, the WT 3′ UTR segments of Notch1 and Rbpj containing the 13_7354-5p binding sites were amplified via PCR and inserted into a pGL3-control vector (Promega, Madison, WI, USA) using the XbaI site, which was immediately downstream of the luciferase stop codon. DNA segments with scrambled target sites (Notch1-MUT and Rbpj-MUT) designed to interfere with seed sequence recognition were also cloned to serve as controls. BM-MSCs were plated in 24-well plates. The cells in each well were transfected with 20 pmol/L 13_7354-5p mimics or NC, 0.8 μg of the firefly luciferase reporter vector, and 0.08 μg of the control vector pRL-TK (Promega) containing Renilla luciferase using Lipofectamine 2000. After 24 h of transfection, firefly and Renilla luciferase activities were measured consecutively using a dual-luciferase reporter assay (Promega) on a Centro LB 960 microplate luminometer (Berthold, Bad Wildbad, Germany). Primers and DNA segments are given in Table S8.

Western Blotting Analysis

Western blotting was performed as previously described.[54] Briefly, total protein was extracted and quantified using a total protein extraction kit (KeyGen, Nanjing, China) and a bicinchoninic acid (BCA) protein assay kit (KeyGen). Next, 30 μg of each sample was separated in 12% SDS polyacrylamide gels and electrophoretically transferred to polyvinylidene fluoride membranes (Millipore, Billerica, MA, USA). After being incubated with 5% BSA in Tris-buffered saline with 0.5% Tween 20, the membranes were incubated at 4°C overnight with primary antibodies against Notch1 (ImmunoWay, USA), Rbpj (Abcam, Cambridge, MA, USA), or Gapdh (Santa Cruz). After the membranes were incubated with horseradish peroxidase-conjugated secondary antibody, the antigen-antibody complexes were visualized using an enhanced chemiluminescence (ECL) kit (Pierce, Rockford, IL, USA). Protein quantification was carried out using FluorChem 2.01 (Alpha Innotech, San Leandro, CA, USA). Protein levels in 13_7354-5p-transfected cells are presented as the fold change normalized to an endogenous reference (Gapdh protein) and relative to NC-transfected cells.

Statistical Analysis

The results are presented as the mean ± SD of at least three separate experiments. Statistical differences between groups were analyzed using one-way ANOVA or a Student's t test. Pearson correlation analysis was used to analyze the correlation between the miRNA expression levels detected by NGS and those detected by qRT-PCR. Statistical analyses were performed using SPSS 16.0 software (SPSS, Chicago, IL, USA). Values of p less than 0.05 were considered statistically significant.

SUPPLEMENTAL INFORMATION

Supplemental Information can be found online at https://doi.org/10.1016/j.omtn.2020.01.001.

AUTHOR CONTRIBUTIONS

F.Z. and X. Liu performed the experiments; F.Z. and Z.W. wrote the paper; H.L., T.Z., and D.H. provided study materials; F.Z., R.W., and X. Lin contributed to data analysis and interpretation; P.S. contributed to collection and assembly of data; and X.P. designed the study and provided final approval of manuscript.

CONFLICTS OF INTEREST

The authors declare no competing interests.

ACKNOWLEDGMENTS

This work was supported by the National Science Foundation of China (nos. 81370883, 81901969, and 81601692), the Shenyang Key Laboratory Project (no. F15-157-1-00), the Key R&D and Technology Transfer Program (no. Z17-5-039), and by the New Teacher Foundation of China Medical University (no. XZR 20160023).

REFERENCES

1. Atkinson, M.A., and Maclaren, N.K. (1994). The pathogenesis of insulin-dependent diabetes mellitus. N. Engl. J. Med. *331*, 1428–1436.
2. Atkinson, M.A., Eisenbarth, G.S., and Michels, A.W. (2014). Type 1 diabetes. Lancet *383*, 69–82.
3. Galivo, F., Benedetti, E., Wang, Y., Pelz, C., Schug, J., Kaestner, K.H., and Grompe, M. (2017). Reprogramming human gallbladder cells into insulin-producing β-like cells. PLoS ONE *12*, e0181812.
4. White, S.L., Rawlinson, W., Boan, P., Sheppeard, V., Wong, G., Waller, K., Opdam, H., Kaldor, J., Fink, M., Verran, D., et al. (2018). Infectious disease transmission in solid organ transplantation: donor evaluation, recipient risk, and outcomes of transmission. Transplant. Direct *5*, e416.
5. Piran, M., Enderami, S.E., Piran, M., Sedeh, H.S., Seyedjafari, E., and Ardeshirylajimi, A. (2017). Insulin producing cells generation by overexpression of miR-375 in adipose-derived mesenchymal stem cells from diabetic patients. Biologicals *46*, 23–28.
6. Li, D.W., He, J., He, F.L., Liu, Y.L., Liu, Y.Y., Ye, Y.J., Deng, X., and Yin, D.C. (2018). Silk fibroin/chitosan thin film promotes osteogenic and adipogenic differentiation of rat bone marrow-derived mesenchymal stem cells. J. Biomater. Appl. *32*, 1164–1173.
7. Hu, T., Xu, H., Wang, C., Qin, H., and An, Z. (2018). Magnesium enhances the chondrogenic differentiation of mesenchymal stem cells by inhibiting activated macrophage-induced inflammation. Sci. Rep. *8*, 3406.
8. Szaraz, P., Gratch, Y.S., Iqbal, F., and Librach, C.L. (2017). In vitro differentiation of human mesenchymal stem cells into functional cardiomyocyte-like cells. J. Vis. Exp. *126*, e55757.
9. Cheng, O., Tian, X., Luo, Y., Mai, S., Yang, Y., Kuang, S., Chen, Q., Ma, J., Chen, B., Li, R., et al. (2017). Liver X receptors agonist promotes differentiation of rat bone marrow derived mesenchymal stem cells into dopaminergic neuron-like cells. Oncotarget *9*, 576–590.
10. Domínguez-Bendala, J., Lanzoni, G., Inverardi, L., and Ricordi, C. (2012). Concise review: mesenchymal stem cells for diabetes. Stem Cells Transl. Med. *1*, 59–63.
11. Abdi, R., Moore, R., Sakai, S., Donnelly, C.B., Mounayar, M., and Sackstein, R. (2015). HCELL expression on murine MSC licenses pancreatotropism and confers durable reversal of autoimmune diabetes in NOD mice. Stem Cells *33*, 1523–1531.
12. Abbasi-Malati, Z., Roushandeh, A.M., Kuwahara, Y., and Roudkenar, M.H. (2018). Mesenchymal stem cells on horizon: a new arsenal of therapeutic agents. Stem Cell Rev Rep *14*, 484–499.
13. Ritfeld, G.J., Nandoe Tewarie, R.D., Vajn, K., Rahiem, S.T., Hurtado, A., Wendell, D.F., Roos, R.A., and Oudega, M. (2012). Bone marrow stromal cell-mediated tissue sparing enhances functional repair after spinal cord contusion in adult rats. Cell Transplant. *21*, 1561–1575.
14. Park, S.S., Moisseiev, E., Bauer, G., Anderson, J.D., Grant, M.B., Zam, A., Zawadzki, R.J., Werner, J.S., and Nolta, J.A. (2017). Advances in bone marrow stem cell therapy for retinal dysfunction. Prog. Retin. Eye Res. *56*, 148–165.
15. Azizi, Z., Lange, C., Paroni, F., Ardestani, A., Meyer, A., Wu, Y., Zander, A.R., Westenfelder, C., and Maedler, K. (2016). β-MSCs: successful fusion of MSCs with β-cells results in a β-cell like phenotype. Oncotarget *7*, 48963–48977.
16. Karnieli, O., Izhar-Prato, Y., Bulvik, S., and Efrat, S. (2007). Generation of insulin-producing cells from human bone marrow mesenchymal stem cells by genetic manipulation. Stem Cells *25*, 2837–2844.
17. Zhang, T., Li, X.H., Zhang, D.B., Liu, X.Y., Zhao, F., Lin, X.W., Wang, R., Lang, H.X., and Pang, X.N. (2017). Repression of COUP-TFI improves bone marrow-derived mesenchymal stem cell differentiation into insulin-producing cells. Mol. Ther. Nucleic Acids *8*, 220–231.
18. Jafarian, A., Taghikhani, M., Abroun, S., Pourpak, Z., Allahverdi, A., and Soleimani, M. (2014). Generation of high-yield insulin producing cells from human bone marrow mesenchymal stem cells. Mol. Biol. Rep. *41*, 4783–4794.
19. Xu, Y., Zhao, F., Wang, Z., Song, Y., Luo, Y., Zhang, X., Jiang, L., Sun, Z., Miao, Z., and Xu, H. (2012). MicroRNA-335 acts as a metastasis suppressor in gastric cancer by targeting Bcl-w and specificity protein 1. Oncogene *31*, 1398–1407.
20. Poy, M.N., Eliasson, L., Krutzfeldt, J., Kuwajima, S., Ma, X., Macdonald, P.E., Pfeffer, S., Tuschl, T., Rajewsky, N., Rorsman, P., and Stoffel, M. (2004). A pancreatic islet-specific microRNA regulates insulin secretion. Nature *432*, 226–230.
21. Poy, M.N., Hausser, J., Trajkovski, M., Braun, M., Collins, S., Rorsman, P., Zavolan, M., and Stoffel, M. (2009). miR-375 maintains normal pancreatic alpha- and beta-cell mass. Proc. Natl. Acad. Sci. USA *106*, 5813–5818.
22. Filios, S.R., and Shalev, A. (2015). β-cell microRNAs: small but powerful. Diabetes *64*, 3631–3644.
23. Jafarian, A., Taghikani, M., Abroun, S., Allahverdi, A., Lamei, M., Lakpour, N., and Soleimani, M. (2015). The generation of insulin producing cells from human mesenchymal stem cells by miR-375 and anti-miR-9. PLoS ONE *10*, e0128650.
24. Bai, C., Gao, Y., Li, X., Wang, K., Xiong, H., Shan, Z., Zhang, P., Wang, W., Guan, W., and Ma, Y. (2017). MicroRNAs can effectively induce formation of insulin-producing cells from mesenchymal stem cells. J. Tissue Eng. Regen. Med. *11*, 3457–3468.
25. Bai, C., Gao, Y., Zhang, X., Yang, W., and Guan, W. (2017). MicroRNA-34c acts as a bidirectional switch in the maturation of insulin-producing cells derived from mesenchymal stem cells. Oncotarget *8*, 106844–106857.
26. Shaer, A., Azarpira, N., and Karimi, M.H. (2014). Differentiation of human induced pluripotent stem cells into insulin-like cell clusters with miR-186 and miR-375 by using chemical transfection. Appl. Biochem. Biotechnol. *174*, 242–258.
27. Ishihara, H., Asano, T., Tsukuda, K., Katagiri, H., Inukai, K., Anai, M., Kikuchi, M., Yazaki, Y., Miyazaki, J.I., and Oka, Y. (1993). Pancreatic beta cell line MIN6 exhibits characteristics of glucose metabolism and glucose-stimulated insulin secretion similar to those of normal islets. Diabetologia *36*, 1139–1145.
28. Baran-Gale, J., Fannin, E.E., Kurtz, C.L., and Sethupathy, P. (2013). Beta cell 5′-shifted isomiRs are candidate regulatory hubs in type 2 diabetes. PLoS ONE *8*, e73240.
29. Friedländer, M.R., Mackowiak, S.D., Li, N., Chen, W., and Rajewsky, N. (2012). miRDeep2 accurately identifies known and hundreds of novel microRNA genes in seven animal clades. Nucleic Acids Res. *40*, 37–52.
30. López-Beas, J., Capilla-González, V., Aguilera, Y., Mellado, N., Lachaud, C.C., Martín, F., Smani, T., Soria, B., and Hmadcha, A. (2018). miR-7 modulates hESC differentiation into insulin-producing beta-like cells and contributes to cell maturation. Mol. Ther. Nucleic Acids *12*, 463–477.
31. Friedländer, M.R., Chen, W., Adamidi, C., Maaskola, J., Einspanier, R., Knespel, S., and Rajewsky, N. (2008). Discovering microRNAs from deep sequencing data using miRDeep. Nat. Biotechnol. *26*, 407–415.

32. Lu, C.J., Fan, X.Y., Guo, Y.F., Cheng, Z.C., Dong, J., Chen, J.Z., Li, L.Y., Wang, M.W., Wu, Z.K., Wang, F., et al. (2019). Single-cell analyses identify distinct and intermediate states of zebrafish pancreatic islet development. J. Mol. Cell Biol. *11*, 435–447.

33. Neelankal John, A., and Jiang, F.X. (2018). An overview of type 2 diabetes and importance of vitamin D3-vitamin D receptor interaction in pancreatic β-cells. J. Diabetes Complications *32*, 429–443.

34. Zhu, Y., Liu, Q., Zhou, Z., and Ikeda, Y. (2017). PDX1, Neurogenin-3, and MAFA: critical transcription regulators for beta cell development and regeneration. Stem Cell Res. Ther. *8*, 240.

35. Jiang, F.X., and Morahan, G. (2012). Pancreatic stem cells: from possible to probable. Stem Cell Rev Rep *8*, 647–657.

36. Dash, S.N., Hakonen, E., Ustinov, J., Otonkoski, T., Andersson, O., and Lehtonen, S. (2016). *sept7b* is required for the differentiation of pancreatic endocrine progenitors. Sci. Rep. *6*, 24992.

37. Jennings, R.E., Berry, A.A., Kirkwood-Wilson, R., Roberts, N.A., Hearn, T., Salisbury, R.J., Blaylock, J., Piper Hanley, K., and Hanley, N.A. (2013). Development of the human pancreas from foregut to endocrine commitment. Diabetes *62*, 3514–3522.

38. Holland, A.M., Hale, M.A., Kagami, H., Hammer, R.E., and MacDonald, R.J. (2002). Experimental control of pancreatic development and maintenance. Proc. Natl. Acad. Sci. USA *99*, 12236–12241.

39. Lee, J., Kim, K., Yu, S.W., and Kim, E.K. (2016). Wnt3a upregulates brain-derived insulin by increasing NeuroD1 via Wnt/β-catenin signaling in the hypothalamus. Mol. Brain *9*, 24.

40. Bartolome, A., Zhu, C., Sussel, L., and Pajvani, U.B. (2019). Notch signaling dynamically regulates adult β cell proliferation and maturity. J. Clin. Invest. *129*, 268–280.

41. Hayward, S.D. (2004). Viral interactions with the Notch pathway. Semin. Cancer Biol. *14*, 387–396.

42. Braune, E.B., and Lendahl, U. (2016). Notch—a goldilocks signaling pathway in disease and cancer therapy. Discov. Med. *21*, 189–196.

43. Jensen, J.N., Cameron, E., Garay, M.V., Starkey, T.W., Gianani, R., and Jensen, J. (2005). Recapitulation of elements of embryonic development in adult mouse pancreatic regeneration. Gastroenterology *128*, 728–741.

44. Baeyens, L., Bonné, S., Bos, T., Rooman, I., Peleman, C., Lahoutte, T., German, M., Heimberg, H., and Bouwens, L. (2009). Notch signaling as gatekeeper of rat acinar-to-β-cell conversion in vitro. Gastroenterology *136*, 1750–60.e13.

45. Anastasi, E., Santangelo, C., Bulotta, A., Dotta, F., Argenti, B., Mincione, C., Gulino, A., Maroder, M., Perfetti, R., and Di Mario, U. (2005). The acquisition of an insulin-secreting phenotype by HGF-treated rat pancreatic ductal cells (ARIP) is associated with the development of susceptibility to cytokine-induced apoptosis. J. Mol. Endocrinol. *34*, 367–376.

46. Hu He, K.H., Lorenzo, P.I., Brun, T., Jimenez Moreno, C.M., Aeberhard, D., Vallejo Ortega, J., Cornu, M., Thorel, F., Gjinovci, A., Thorens, B., et al. (2011). In vivo conditional Pax4 overexpression in mature islet β-cells prevents stress-induced hyperglycemia in mice. Diabetes *60*, 1705–1715.

47. Liu, X., Wang, Z., Wang, R., Zhao, F., Shi, P., Jiang, Y., and Pang, X. (2013). Direct comparison of the potency of human mesenchymal stem cells derived from amnion tissue, bone marrow and adipose tissue at inducing dermal fibroblast responses to cutaneous wounds. Int. J. Mol. Med. *31*, 407–415.

48. Zhao, F., Wang, Z., Lang, H., Liu, X., Zhang, D., Wang, X., Zhang, T., Wang, R., Shi, P., and Pang, X. (2015). Dynamic expression of novel miRNA candidates and miRNA-34 family members in early- to mid-gestational fetal keratinocytes contributes to scarless wound healing by targeting the TGF-β pathway. PLoS ONE *10*, e0126087.

49. Wu, P., Han, S., Chen, T., Qin, G., Li, L., and Guo, X. (2013). Involvement of microRNAs in infection of silkworm with *Bombyx mori* cytoplasmic polyhedrosis virus (BmCPV). PLoS ONE *8*, e68209.

50. Burge, S.W., Daub, J., Eberhardt, R., Tate, J., Barquist, L., Nawrocki, E.P., Eddy, S.R., Gardner, P.P., and Bateman, A. (2013). Rfam 11.0: 10 years of RNA families. Nucleic Acids Res. *41*, D226–D232.

51. Pruesse, E., Quast, C., Knittel, K., Fuchs, B.M., Ludwig, W., Peplies, J., and Glöckner, F.O. (2007). SILVA: a comprehensive online resource for quality checked and aligned ribosomal RNA sequence data compatible with ARB. Nucleic Acids Res. *35*, 7188–7196.

52. Bao, W., Kojima, K.K., and Kohany, O. (2015). Repbase Update, a database of repetitive elements in eukaryotic genomes. Mob. DNA *6*, 11.

53. Robinson, M.D., McCarthy, D.J., and Smyth, G.K. (2010). edgeR: a Bioconductor package for differential expression analysis of digital gene expression data. Bioinformatics *26*, 139–140.

54. Zhao, F., Lang, H., Wang, Z., Zhang, T., Zhang, D., Wang, R., Lin, X., Liu, X., Shi, P., and Pang, X. (2019). Human novel microRNA Seq-915_x4024 in keratinocytes contributes to skin regeneration by suppressing scar formation. Mol. Ther. Nucleic Acids *14*, 410–423.